Motion Control Design of UNUSAITS AUV Using Sliding PID

T. Herlambang [1], S. Subchan [2*], H. Nurhadi [3,4] and D. Adzkiya [2,4]

[1] *Department of Information Systems, University of Nahdlatul Ulama Surabaya, Indonesia*
[2] *Department of Mathematics, Sepuluh Nopember Institute of Technology, Indonesia*
[3] *Department of Industrial Mechanical Engineering, Sepuluh Nopember Institute of Technology, Indonesia*
[4] *Center of Excellence for Mechatronics and Industrial Automation Research Center, Sepuluh Nopember Institute of Technology, Indonesia*

Abstract: An unmanned submarine commonly called an Autonomous Underwater Vehicle (AUV) is one type of underwater robots used for underwater mapping. The AUV is an underwater vehicle capable of automatically moving in the water, controlled by humans on a vessel. Building an AUV is not easy as many components play important roles in the operation of the AUV. One of them is the motion control system. This paper develops the motion control system of the UNUSAITS AUV by applying a Sliding PID (SPID) control to a linear model with 6-DOF. The linear model is obtained through linearization of the nonlinear model with 6-DOF. The SPID is a combination of the Sliding Mode Control (SMC) and PID. The results of the study indicate that the SPID method can be effectively used as the motion control system of the linear model with an error of 0.2% - 4.2%.

* Corresponding author: mailto:subchan@matematika.its.ac.id

1   Introduction

Underwater vehicle technology plays an important role for archipelago nations such as Indonesia. Since its water area is much larger than its land area, underwater technology is required to explore and keep or maintain its natural resources. So, an underwater vehicle is needed [1]. Underwater rides widely developed by many researchers and practitioners today are unmanned underwater robots. This robot is known as the Autonomous Underwater Vehicle (AUV). The AUV is one type of underwater robots that have attracted a lot of researchers in recent years [2]. The AUV is a vehicle driven through water with a propulsion system, controlled and driven by an onboard computer with six degrees of freedom (DOF) maneuver, so that it can carry out its determined tasks entirely by itself. The benefits of the AUV are not only for exploring marine resources, but also for underwater mapping and underwater defense system equipment [3, 4].

Several studies on the AUV control system that have been conducted within the period of 1990s up to now can be described as follows. Guo, Chiu and Huang examined the AUV motion control by using a Fuzzy Sliding Mode Control for 6-DOF [5]. Then, Mc Gann et al. used an adaptive control for 6-DOF underwater vehicles [6]. Petric dan Stilwell applied PID to the Virginia Tech 475 AUV model with 2-DOF [7]. Oktafianto et al. developed a Sliding Mode Control (SMC) method for a 6-DOF linear model [8]. Herlambang et al. proposed a Particle Swarm Optimization (PSO) and Ant Colony Optimization (ACO) for controlling an AUV system [9].

This study was carried out in the following stages. First, the equation of motion for the 6-DOF nonlinear model was formulated. Then, the model was linearized using the Jacobi matrix to obtain the 6-DOF linear model. Next, the Sliding PID (SPID) method was employed to control the motion of the 6-DOF model to reach the desired set point in the disturbance-free case (when the AUV is moving).

2   Autonomous Underwater Vehicle

Two important things are considered essential to analyze an AUV, that is, the axis system consisting of the Earth Fixed Frame (EFF) and Body Fixed Frame (BFF) as seen in Figure 1 (left) [10]. The EFF is used to show the position and orientation of the AUV, of which the x-axis position leads northward, the y-axis goes to the east, and the z-axis heads toward the center of the earth. The BFF defines the positive x-axis leading to the prowess of the vehicle, the positive y-axis leads to the right side of the vehicle, and the positive z-axis points downward [10]. The BFF system is used to show the speed and acceleration of the AUV with the starting point at the center of gravity. The profile of the UNUSAITS AUV is shown in Figure 1 (right). Figure 1 (left) and Table 1 show that the AUV has six degrees of freedom (6-DOF), that is, surge, sway, heave, roll, pitch and yaw. The equation of AUV motion is influenced by the outer force as follows:

$$\tau = \tau_{hydrostatic} + \tau_{addedmass} + \tau_{drag} + \tau_{lift} + \tau_{control}.$$

The movement of the UNUSAITS AUV has 6 degrees of freedom, that is, 3 (three) degrees of freedom for the direction of translational motion on the x-axis (surge), y-axis (sway), and z-axis (heave) and the other 3 (three) degrees of freedom for rotational motion on the x-axis (roll), y-axis (yaw), and z-axis (pitch). The UNUSAITS AUV specifications include, among others, weight of 16 kg, length of 1.5 m, and a diameter of 20 cm [12]. The general description of the AUV with 6 DOF can be expressed in the
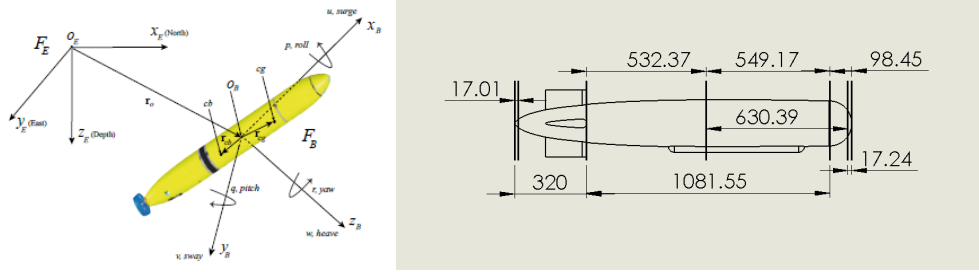
Figure 1: AUV motion with six degrees of freedom [11] and profile of UNUSAITS AUV [12].

Weight	16 Kg
Length	1500 mm
Diameter	200 mm
Controller	Ardupilot Mega 2.0
Communication	Wireless Xbee 2.4 GHz
Camera	TTL Camera
Battery	Li-Pro 11.8 V
Propulsion	12 V DC motor
Propeller	3 Blades OD : 50 mm
Speed	3.1 knots (1.5 m/s)
Maximum depth	8 m

Table 1: Specification of UNUSAITS AUV.

equations [10]:

$$\eta = [\eta_1^T, \eta_2^T]^T, \qquad \eta_1 = [x, y, z]^T, \qquad \eta_2 = [\phi, \theta, \psi]^T;$$
$$v = [v_1^T, v_2^T]^T, \qquad v_1 = [u, v, w]^T, \qquad v_2 = [p, q, r]^T;$$
$$\tau = [\tau_1^T, \tau_2^T]^T, \qquad v_1 = [X, Y, Z]^T, \qquad v_2 = [K, M, N]^T;$$

In the equations above, η shows the vector position and orientation on the EFF. Then, τ denotes the force vector and moment working on the AUV on the BFF, namely, surge (u), sway (v), heave (w), roll (p), pitch (q) and yaw (r). The total force and moment working on the AUV can be obtained by combining hydrostatic forces, hydrodynamic forces and thrust forces. In this case, it is assumed that the diagonal inertia tensor (I_o) is zero, to obtain the total force and moment of the whole nonlinear AUV model [2]. The following equations represent the surge, sway, heave, roll, pitch and yaw motions, respectively:

$$m[\dot{u} - vr + wq - x_G(q^2 + r^2) + y_G(pq - \dot{r}) + z_G(pr + \dot{q})] = X_{res} + X_{|u|u}u|u| + X_{\dot{u}}\dot{u}$$
$$+ X_{wq}wq + X_{qq}qq + X_{vr}vr + X_{rr}rr + X_{prop}, \tag{1}$$
$$m[\dot{v} - wp + ur - y_G(r^2 + p^2) + z_G(qr - \dot{p}) + x_G(pq + \dot{r})] = Y_{res} + Y_{|v|v}v|v| + Y_{r|r|}r|r|$$

$$+ Y_{\dot{v}}\dot{v} + Y_{\dot{r}}\dot{r} + Y_{ur}ur + Y_{wp}wp + Y_{pq}pq + Y_{uv}uv + Y_{uu\delta_{r1}}u^2\delta_{r1}, \tag{2}$$

$$m[\dot{w} - uq + vp - z_G(p^2 + q^2) + x_G(rp - \dot{q}) + y_G(rq + \dot{p})] = Z_{res} + Z_{|w|w}w|w|$$
$$+ Z_{q|q|}q|q| + Z_{\dot{w}}\dot{w} + Z_{\dot{q}}\dot{q} + Z_{uq}uq + Z_{vp}vp + Z_{rp}rp + Z_{uw}uw + Z_{uu\delta_{s1}}u^2\delta_{s1}, \tag{3}$$

$$I_x\dot{p} + (I_z - I_y)qr + m[y_G(\dot{w} - uq + vp) - z_G(\dot{v} - wp + ur)] = K_{res} + K_{p|p|}p|p| + K_{\dot{p}}\dot{p}$$
$$+ K_{prop}, \tag{4}$$

$$I_y\dot{q} + (I_x - I_z)rp + m[z_G(\dot{u} - vr + wq) - x_G(\dot{w} - uq + vp)] = M_{res} + M_{w|w|}w|w|$$
$$+ M_{q|q|}q|q| + M_{\dot{w}}\dot{w} + M_{\dot{q}}\dot{q} + M_{uq}uq + M_{vp}vp + M_{rp}rp + M_{uw}uw + M_{uu\delta_{s2}}u^2\delta_{s2}, \tag{5}$$

$$I_z\dot{r} + (I_y - I_z)pq + m[x_G(\dot{v} - wp + ur) - y_G(\dot{u} - vr + wq)] = N_{res} + N_{v|v|}v|v|$$
$$+ N_{r|r|}r|r| + N_{\dot{v}}\dot{v} + N_{\dot{r}}\dot{r} + N_{ur}ur + N_{wp}wp + N_{pq}pq + N_{uv}uv + N_{uu\delta_{r2}}u^2\delta_{r2}. \tag{6}$$

The state variables of the model in (1)-(6) are u (surge), v (sway), w (heave), p (roll), q (pitch) and r (yaw), i.e., $x = [u, v, w, p, q, r]^T$. In this work, we assume that all state variables are measured, i.e., $y = x$. The input variables are X_{prop}, δ_{r1}, δ_{s1}, K_{prop}, δ_{s2} and δ_{r2}, i.e., $u = [X_{prop}, \delta_{r1}, \delta_{s1}, K_{prop}, \delta_{s2}, \delta_{r2}]^T$. It follows that the model in (1)-(6) can be formulated in the following state-space form:

$$\dot{x}(t) = f(x(t), u(t), t), \tag{7}$$
$$y(t) = x(t), \tag{8}$$

where

$$f_1(x, u) = (-m[-vr + wq - x_G(q^2 + r^2) + pqy_G + prz_G] + X_{res} + X_{|u|u}u|u| + X_{wq}wq$$
$$+ X_{qq}qq + X_{vr}vr + X_{rr}rr + X_{prop})/(m - X_{\dot{u}}), \tag{9}$$

$$f_2(x, u) = (-m[-wp + ur - y_G(r^2 + p^2) + qrz_G + pqx_G] + Y_{res} + Y_{|v|v}v|v| + Y_{r|r|}r|r|$$
$$+ Y_{\dot{r}}\dot{r} + Y_{ur}ur + Y_{wp}wp + Y_{pq}pq + Y_{uv}uv + Y_{uu\delta_{r1}}u^2\delta_{r1})/(m - Y_{\dot{v}}), \tag{10}$$

$$f_3(x, u) = (-m[-uq + vp - z_G(p^2 + q^2) + rpx_G + rqy_G] + Z_{res} + Z_{|w|w}w|w| + Z_{q|q|}q|q|$$
$$+ Z_{\dot{q}}\dot{q} + Z_{uq}uq + Z_{vp}vp + Z_{rp}rp + Z_{uw}uw + Z_{uu\delta_{s1}}u^2\delta_{s1})/(m - Z_{\dot{w}}), \tag{11}$$

$$f_4(x, u) = (-(I_z - I_y)qr - m[y_G(-uq + vp) - z_G(-wp + ur)] + K_{res} + K_{p|p|}p|p|$$
$$+ K_{prop})/(I_x - K_{\dot{p}}), \tag{12}$$

$$f_5(x, u) = (-(I_x - I_z)rp - m[z_G(-vr + wq) - x_G(-uq + vp)] + M_{res} + M_{w|w|}w|w|$$
$$+ M_{q|q|}q|q| + M_{\dot{w}}\dot{w} + M_{uq}uq + M_{vp}vp + M_{rp}rp + M_{uw}uw + M_{uu\delta_{s2}}u^2\delta_{s2})$$
$$/(I_y - M_{\dot{q}}), \tag{13}$$

$$f_6(x, u) = (-(I_y - I_z)pq - m[x_G(-wp + ur) - y_G(-vr + wq)] + N_{res} + N_{v|v|}v|v|$$
$$+ N_{r|r|}r|r| + N_{\dot{v}}\dot{v} + N_{ur}ur + N_{wp}wp + N_{pq}pq + N_{uv}uv + N_{uu\delta_{r2}}u^2\delta_{r2})$$
$$/(I_z - N_{\dot{r}}). \tag{14}$$

Notice that the nonlinear AUV model in (7)-(8) is quite complicated. Thus, it is difficult to design a controller for the nonlinear model. Therefore, we linearize the nonlinear AUV model (7)-(8) around a solution by using the Jacobi matrix. The linearized AUV model is given by

$$\dot{x}(t) = Ax(t) + Bu(t), \tag{15}$$

$$y(t) = Cx(t) + Du(t), \tag{16}$$

where

$$
A = \begin{bmatrix}
1 & 0 & 0 & 0 & \frac{mz_G}{m-X_{\dot u}} & \frac{-my_G}{m-X_{\dot u}} \\
0 & 1 & 0 & -\frac{mz_G}{m-Y_{\dot v}} & 0 & \frac{mx_G-Y_{\dot r}}{m-Y_{\dot v}} \\
0 & 0 & 1 & \frac{my_G}{m-Z_{\dot w}} & \frac{(mx_G+Z_{\dot q})}{m-Z_{\dot w}} & 0 \\
0 & -\frac{mz_G}{I_x-K_{\dot p}} & \frac{my_G}{I_x-K_{\dot p}} & 1 & 0 & 0 \\
\frac{mz_G}{I_y-M_{\dot q}} & 0 & -\frac{(mx_G+M_{\dot w})}{I_y-M_{\dot q}} & 0 & 1 & 0 \\
-\frac{my_G}{I_z-N_{\dot r}} & \frac{mx_G-N_{\dot v}}{I_z-N_{\dot r}} & 0 & 0 & 0 & 1
\end{bmatrix}^{-1}
$$
$$
\begin{bmatrix}
a_1 & b_1 & c_1 & d_1 & e_1 & g_1 \\
a_2 & b_2 & c_2 & d_2 & e_2 & g_2 \\
a_3 & b_3 & c_3 & d_3 & e_3 & g_3 \\
a_4 & b_4 & c_4 & d_4 & e_4 & g_4 \\
a_5 & b_5 & c_5 & d_5 & e_5 & g_5 \\
a_6 & b_6 & c_6 & d_6 & e_6 & g_6
\end{bmatrix}, \tag{17}
$$

$$
B = \begin{bmatrix}
1 & 0 & 0 & 0 & \frac{mz_G}{m-X_{\dot u}} & \frac{-my_G}{m-X_{\dot u}} \\
0 & 1 & 0 & -\frac{mz_G}{m-Y_{\dot v}} & 0 & \frac{mx_G-Y_{\dot r}}{m-Y_{\dot v}} \\
0 & 0 & 1 & \frac{my_G}{m-Z_{\dot w}} & \frac{(mx_G+Z_{\dot q})}{m-Z_{\dot w}} & 0 \\
0 & -\frac{mz_G}{I_x-K_{\dot p}} & \frac{my_G}{I_x-K_{\dot p}} & 1 & 0 & 0 \\
\frac{mz_G}{I_y-M_{\dot q}} & 0 & -\frac{(mx_G+M_{\dot w})}{I_y-M_{\dot q}} & 0 & 1 & 0 \\
-\frac{my_G}{I_z-N_{\dot r}} & \frac{mx_G-N_{\dot v}}{I_z-N_{\dot r}} & 0 & 0 & 0 & 1
\end{bmatrix}^{-1}
$$
$$
\begin{bmatrix}
A_1 & B_1 & C_1 & D_1 & E_1 & G_1 \\
A_2 & B_2 & C_2 & D_2 & E_2 & G_2 \\
A_3 & B_3 & C_3 & D_3 & E_3 & G_3 \\
A_4 & B_4 & C_4 & D_4 & E_4 & G_4 \\
A_5 & B_5 & C_5 & D_5 & E_5 & G_5 \\
A_6 & B_6 & C_6 & D_6 & E_6 & G_6
\end{bmatrix}, \tag{18}
$$

$$
C = \begin{bmatrix}
1 & 0 & 0 & 0 & 0 & 0 \\
0 & 1 & 0 & 0 & 0 & 0 \\
0 & 0 & 1 & 0 & 0 & 0 \\
0 & 0 & 0 & 1 & 0 & 0 \\
0 & 0 & 0 & 0 & 1 & 0 \\
0 & 0 & 0 & 0 & 0 & 1
\end{bmatrix}, \qquad
D = \begin{bmatrix}
0 & 0 & 0 & 0 & 0 & 0 \\
0 & 0 & 0 & 0 & 0 & 0 \\
0 & 0 & 0 & 0 & 0 & 0 \\
0 & 0 & 0 & 0 & 0 & 0 \\
0 & 0 & 0 & 0 & 0 & 0 \\
0 & 0 & 0 & 0 & 0 & 0
\end{bmatrix}. \tag{19}
$$

3 Sliding PID

The Sliding-PID control system design is a combination of the SMC and PID. In the first stage, the error signal (the difference between the set point and the output) is used

as an input to the SMC. The SMC produces a signal that will guarantee that the error becomes zero in finite time. Then, the signal generated by the SMC is used as an input to the PID. Finally, the PID generates a signal that will be sent to the model as the input signal. The above process can be compactly displayed as a block diagram of the Sliding PID in Figure 2.
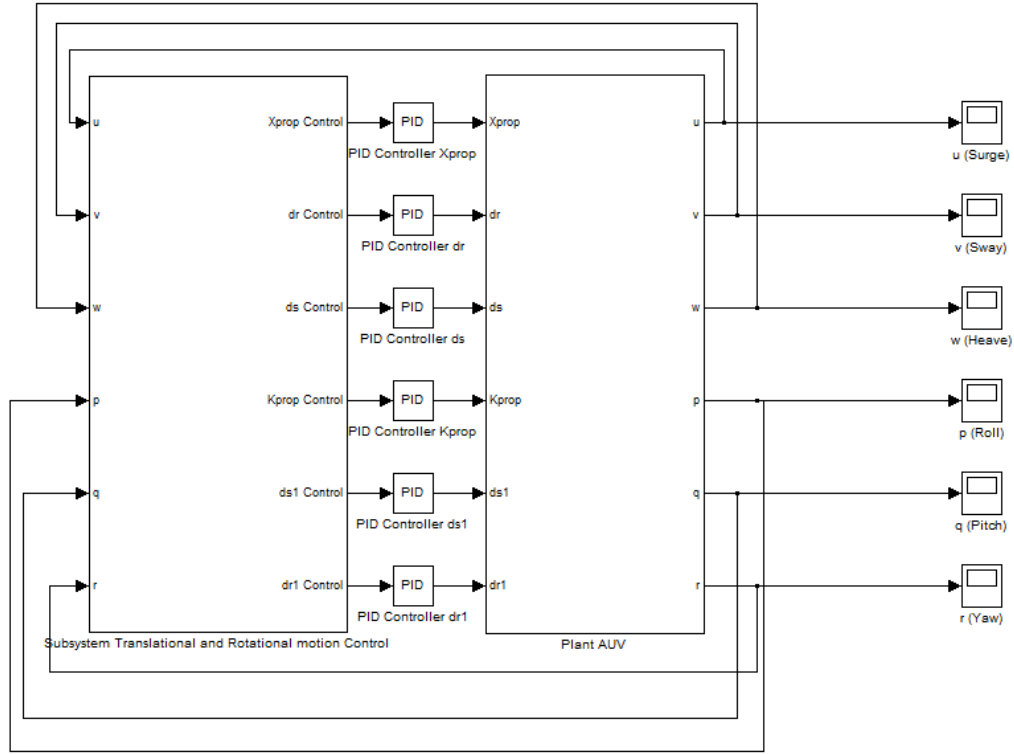

Figure 2: The block diagram of SPID.

Next, we design the SMC control system of the 6-DOF linear model for surge, sway, heave, roll, pitch and yaw. The SMC algorithm is used to compute the control input for those motions. Without going into the details, the control law produced by the SMC for each motion is as follows:

$$X_{prop} = -\left(\frac{aa_1 u + bb_1 v + cc_1 w + dd_1 p + ee_1 q + gg_1 r + BB_1 \delta_{r1} + CC_1 \delta_{s1}}{AA_1} \right)$$
$$- \left(\frac{DD_1 K_{prop} + EE_1 \delta_{s2} + GG_1 \delta_{r2}}{AA_1} \right) - \left| \max \frac{\eta}{AA_1} \right| \, \text{sat} \left(\frac{S}{\phi} \right), \tag{20}$$

$$\delta_{r1} = -\left(\frac{aa_2 u + bb_2 v + cc_2 w + dd_2 p + ee_2 q + gg_2 r + AA_2 X_{prop} + CC_2 \delta_{s1}}{BB_2} \right)$$
$$- \frac{DD_2 K_{prop} + EE_2 \delta_{s2} + GG_2 \delta_{r2}}{BB_2} - \left| \max \frac{\eta}{BB_2} \right| \, \text{sat} \left(\frac{S}{\phi} \right), \tag{21}$$

$$\delta_{s1} = -\left(\frac{aa_3u + bb_3v + cc_3w + dd_3p + ee_3q + gg_3r + AA_3X_{prop} + BB_3\delta_{r1}}{CC_3}\right)$$
$$-\left(\frac{DD_3K_{prop} + EE_3\delta_{s2} + GG_3\delta_{r2}}{CC_3}\right) - \left|\max\frac{\eta}{CC_3}\right| \operatorname{sat}\left(\frac{S}{\phi}\right), \tag{22}$$

$$K_{prop} = -\left(\frac{aa_4u + bb_4v + cc_4w + dd_4p + ee_4q + gg_4r + AA_4X_{prop} + BB_4\delta_{r1}}{DD_4}\right)$$
$$-\left(\frac{CC_4\delta_{s1} + EE_4\delta_{s2} + GG_4\delta_{r2}}{DD_4}\right) - \left|\max\frac{\eta}{AA_1}\right| \operatorname{sat}\left(\frac{S}{\phi}\right), \tag{23}$$

$$\delta_{s2} = -\left(\frac{aa_5u + bb_5v + cc_5w + dd_5p + ee_5q + gg_5r + AA_3X_{prop} + BB_5\delta_{r1} + CC_5\delta_{s1}}{EE_5}\right)$$
$$-\left(\frac{DD_5K_{prop} + GG_5\delta_{r2}}{EE_5}\right) - \left|\max\frac{\eta}{CC_3}\right| \operatorname{sat}\left(\frac{S}{\phi}\right), \tag{24}$$

$$\delta_{r2} = -\left(\frac{aa_6u + bb_6v + cc_6w + dd_6p + ee_6q + gg_6r + AA_6X_{prop} + BB_6\delta_{r1} + CC_6\delta_{s1}}{GG_6}\right)$$
$$-\left(\frac{DD_6K_{prop} + EE_6\delta_{s2}}{GG_6}\right) - \left|\max\frac{\eta}{BB_2}\right| \operatorname{sat}\left(\frac{S}{\phi}\right). \tag{25}$$

As shown in Figure 2, the signals generated by the SMC (20)-(25) are fed to the PID controller. In the PID controller, the coefficients for the proportional, integral and derivative terms are shown in Table 2.

	K_p	K_i	K_d
Surge	3.1	0	0
Sway	2.5	0	0
Heave	2.5	0	0
Roll	2.04	0	0
Pitch	2.2	0	0
Yaw	2.2	0	0

Table 2: The coefficients of the proportional, integral and derivative terms.

The designing the SPID control system on the 6-DOF linear model first passes the SMC control system equation then optimized by the PID controller, of which the proportional, integral and derivative values are shown in Table 2. Once the control system equations are obtained, then they are connected to the 6-DOF linear model on the block diagram shown by Figure 2.

4   Computational Results

In this section, we present the simulation results of the closed-loop system by using the SPID controller designed in the previous section. First of all, we define the set point for surge, sway, heave, roll, pitch and yaw. The set point of surge, sway and heave is 1 m/s. The set point for roll rotation motion is 1 rad/s, whereas those of pitch and yaw are -1 rad/s. For each simulation result, we compare the time delay, rise time, peak time and settling time. The simulation results by using SPID control systems are as shown in Figure 3.
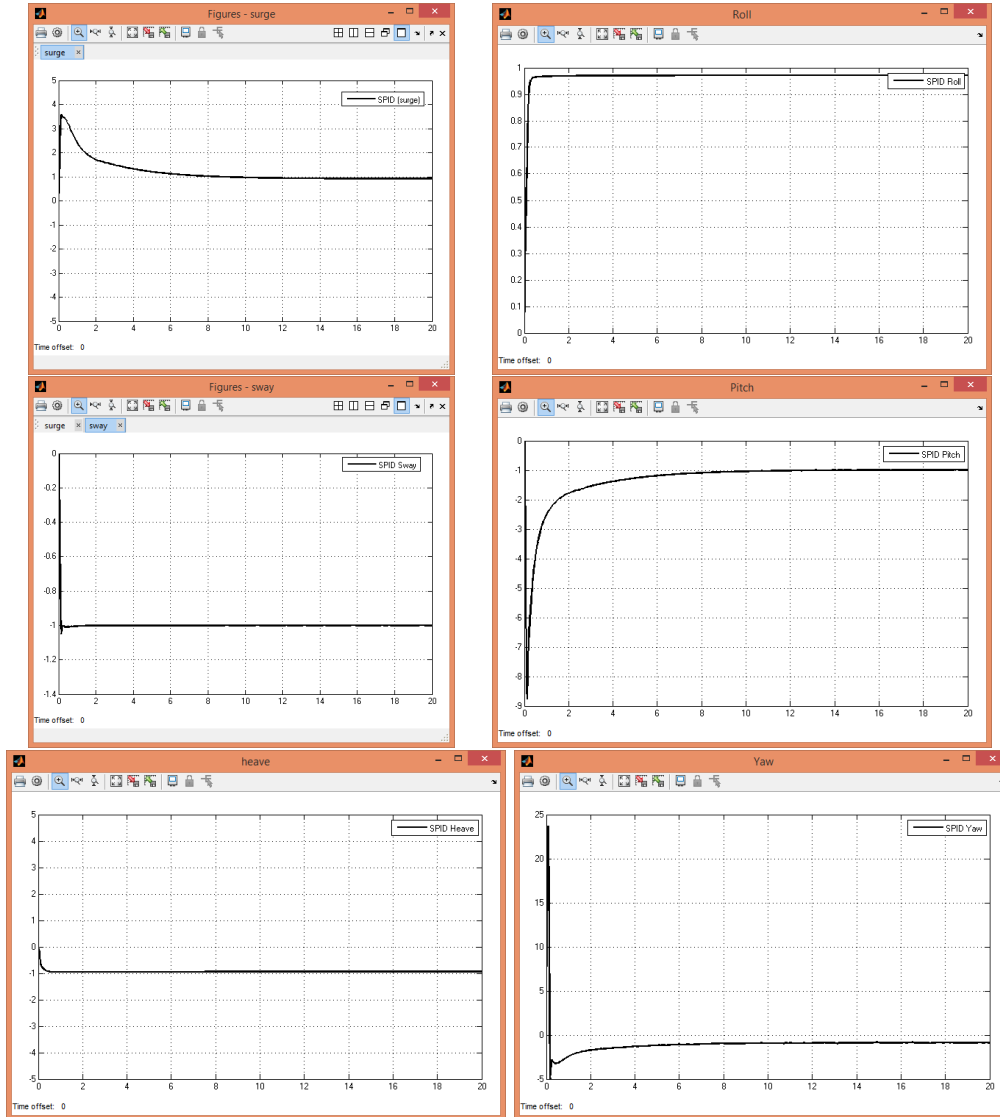
Figure 3: The results of the simulation by using the Sliding PID control system for surge and sway.

Figure 3 shows that the surge responses by the SPID were more stable at a set point of 1 m/s, reaching a settling time in 6 seconds with a maximum overshoot of 3.5 m/s, and had an error of 3.2%. The sway response is stable at the set point of −1 m/s, reaching the settling time in 0.1 of a second, and having an error of 0.1%. The heave response is also stable at the set point of −1 m/s, reaching a settling time in approximately 0.2 of a second, and having an error of 0.2%. These results show that the responses generated by the SPID in surge, sway, and heave motion were stable for surge, sway and heave motions. In this case, the overshoot was not the main consideration for the autonomous platform

performance. The prioritized ones were the settling time and the resulting error.

The results of simulation for rotational motion are shown in Figure 3. For the roll response, the result of simulation with the SPID shows that the roll responses were stable at the set point of 1 rad/s, reached a settling time in 0.15 of a second with a maximum overshoot of 1.2 rad/s, and had an error of 0.5%. The pitch responses by the SPID were also stable at set point of −1 rad/s, reached a settling time in 1.5 of a second with a maximum overshoot of −4.8 rad/s, and had an error of 4.1%. Finally, the yaw responses by the SPID were stable at the set point of −1 rad/s, reached a settling time in 0.25 of a second with a maximum overshoot of −5.6 rad/s, and had an error of 4.2%. In summary, the responses by the SPID in roll, pitch, and yaw were stable. The complete results of the transient responses are shown in Table 3, which shows that the error is very small.

	Surge	Sway	Heave	Roll	Pitch	Yaw
Delay time	0.04 s	0.042 s	0.043 s	0.045 s	0.09 s	0.003 s
Rise time	0.06 s	0.07 s	0.3 s	0.18 s	1.4 s	0.09 s
Peak time	0.1 s	0.01 s	0 s	0 s	0.3 s	0.1 s
Maximum peak	3.5 m/s	-1.08 m/s	0 m/s	0 m/s	-4.8 m/s	-5.6 m/s
Settling time	6 s	0.1 s	0.2 s	0.15 s	1.5 s	0.25 s
Error	3.2 %	0.1 %	0.2 %	0.5 %	4.1 %	4.2 %

Table 3: Specification of the transient responses in surge, sway, heave, roll, pitch, and yaw motions.

5   Conclusion

Based on the results of simulation and discussion about designing the Sliding Proportional, Integral, and Derivative (SPID) control system, regarding the linear model of 6-DOF, it could be concluded that the SPID method could be used as a motion control system of the 6-DOF linear model with a significant accuracy and an error of about 0.2% − 4.2%.

References

[1] T. Herlambang, H. Nurhadi and Subchan. Preliminary Numerical Study on Designing Navigation and Stability Control Systems for ITS AUV. *Applied Mechanics and Materials* **493** (2014) 420–452.

[2] T. Herlambang, E. B. Djatmiko and H. Nurhadi. Ensemble Kalman filter with a square root scheme (enkf-sr) for trajectory estimation of AUV SEGOROGENI ITS. *International Review of Mechanical Engineering* **9** (6) (2015) 553–560.

[3] T. Herlambang, E. B. Djatmiko and H. Nurhadi. Navigation and guidance control system of AUV with trajectory estimation of linear modelling. In: *Proc. International Conf. on Advanced Mechatronics, Intelligent Manufacture, and Industrial Automation (ICAMIMIA)* Surabaya, Indonesia, 2015, 184–187.

[4] Z. Ermayanti, E. Apriliani, H. Nurhadi and T. Herlambang. Estimate and control position autonomous underwater vehicle based on determined trajectory using fuzzy Kalman filter method. In: *Proc. International Conf. on Advanced Mechatronics, Intelligent Manufacture, and Industrial Automation (ICAMIMIA)* Surabaya, Indonesia, 2015, 156–161.

[5] J. Guo, F.-C. Chiu and C.-C. Huang. Design of a sliding mode fuzzy controller for the guidance and control of an autonomous underwater vehicle. *Ocean Engineering* **30** (16) (2003) 2137–2155.

[6] C. McGann, F. Py, K. Rajan, J. P. Ryan and R. Henthorn. Adaptive control for autonomous underwater vehicles. In: *Proc. Twenty-Third AAAI Conf. on Artificial Intelligence* 2008, 1319–1324.

[7] J. Petrich and D. J. Stilwell. Model simplification for AUV pitch-axis control design. *Ocean Engineering* **37** (7) (2010) 638–651.

[8] K. Oktafianto, T. Herlambang, Mardlijah and H. Nurhadi. Design of Autonomous Underwater Vehicle motion control using Sliding Mode Control method. In: *Proc. International Conf. on Advanced Mechatronics, Intelligent Manufacture, and Industrial Automation (ICAMIMIA)* Surabaya, Indonesia, 2015, 162–166.

[9] T. Herlambang, D. Rahmalia and T. Yulianto. Particle Swarm Optimization (PSO) and Ant Colony Optimization (ACO) for Optimizing PID Parameters on Autonomous Underwater Vehicle (AUV) Control System. *Journal of Physics: Conference Series* **1211** (1) (2019) 012039.

[10] C. Yang. Modular modelling and control for autonomous vehicle (AUV). *Department of Mechanical Engineering National University of Singapore* (2007).

[11] U. Ansari and A. H. Bajodah. Robust generalized dynamic inversion control of autonomous underwater vehicles. *IFAC-PapersOnLine* **50** (1) (2017) 10658–10665.

[12] T. Herlambang, S. Subchan and H. Nurhadi. Design of Motion Control Using Proportional Integral Derivative for UNUSAITS AUV. *International Review of Mechanical Engineering (IREME)* **12** (11) (2018) 928–938.